

# Long-term Geochemical Evolution of Lithogenic Versus Anthropogenic Distribution of Macro and Trace Elements in Household Attic Dust

Biljana Balabanova<sup>1</sup> · Trajče Stafilov<sup>2</sup>  · Robert Šajn<sup>3</sup> · Claudiu Tănăselia<sup>4</sup>

Received: 27 July 2016 / Accepted: 17 November 2016 / Published online: 29 November 2016  
© Springer Science+Business Media New York 2016

**Abstract** Attic dusts were examined as historical archives of anthropogenic emissions, with the goal of elucidating the enrichment pathways associated with hydrothermal exploitation of Cu, Pb, and Zn minerals in the Bregalnica River basin in the eastern part of the Republic of Macedonia. Dust samples were collected from 84 settlements. Atomic emission spectrometry and mass spectrometry with inductively coupled plasma were applied as analytical techniques for the determination of 69 element contents. Multivariate analysis was applied for the extraction of dominant geochemical markers. The lithogenic distribution was simplified to six dominant geochemical markers: F1: Ga–Nb–Ta–Y–(La–Gd)–(Eu–Lu); F2: Be–Cr–Li–Mg–Ni; F3: Ag–Bi–Cd–Cu–In–Mn–Pb–Sb–Te–W–Zn; F4: Ba–Cs–Hf–Pd–Rb–Sr–Tl–Zr; F5: As–Co–Ge–V; and F6: K–Na–Sc–Ti. The anthropogenic effects on the air pollution were marked by a dominance of F3 and secondary dominance of F5. The fifth factor also was determined as a lithogenic marker for the occurrence of the very old Rifeous shales. The first factor also presents a very unique association that despite the heterogeneity relays on natural phenomena of tracking the deposition in areas of Proterozoic gneisses; related to the distribution of fine particles was associated

with carbonate–silicate volcanic rocks. Intensive poly-metallic dust depositions were recorded only in the surroundings of localities where the hydrothermal extractions are implemented. Long-term deposition can be considered as pollution indexes for these hot spots. This mainly affects the Cd, Pb, and Zn deposition that is as high as 25, 3900, and 3200 mg/kg, respectively.

Atmospheric deposition poses significant ecological concerns. According to the process of deposition, particles can be deposited at the Earth's surface in two ways: dry or wet deposition, depending on the phase in which a species strikes the Earth's surface and is taken up (Finlayson-Pitts and Pitts 1999). Dry deposition is characterised by the direct transfer of gas phase and particulates from the air to the ground, vegetation, water bodies, and other Earth surfaces (White 2013). This transfer can occur by sedimentation, impaction, and diffusion to surfaces or in case of plants by physiological uptake (Mulligan 2009; Davis and Gulson 2005). In the absence of precipitation, dry deposition plays a major role in removing pollutants from the atmosphere (Finlayson-Pitts and Pitts 1999). Atmospheric particles originate both from natural (e.g., erosion, dust storm, volcanoes) and anthropogenic sources. (e.g., fuel combustion, mining, metal industries, traffic, coal-fired power plants (Davis and Gulson 2005; Alijagić 2008; Ajmone-Marsan et al. 2008; Neff et al. 2008; Gosar and Teršič 2012). The Macedonian post-war centrally directed economy led to heavy industry to producing large amounts of waste and emissions, leading to related air pollution (Stafilov et al. 2012; Stafilov 2014). Long-term airborne emissions from mining, power plants, smelting and industry have left a legacy of widespread contamination around industrial areas (Balabanova et al.

✉ Trajče Stafilov  
trajcest@pmf.ukim.mk

<sup>1</sup> Faculty of Agriculture, University “Goce Delčev”, Krste Misirkov bb, Štip, Republic of Macedonia

<sup>2</sup> Institute of Chemistry, Faculty of Science, Ss. Cyril and Methodius University, POB 162, 1000 Skopje, Macedonia

<sup>3</sup> Geological Survey of Slovenia, Dimičeva ulica 14, 1000 Ljubljana, Slovenia

<sup>4</sup> INCDO-INOE 2000 Research Institute for Analytical Instrumentation (ICIA), Cluj-Napoca, Romania

2010, 2011, 2012, 2014, 2015, 2016; Bačeva et al. 2012; Stafilov 2014; Barandovski et al. 2015; Angelovska et al. 2016). The Eastern part (Bregalnica River basin) of the country is significantly affected due to the major emissions from the Pb–Zn Sasa mine, Pb–Zn Zletovo mine, Cu–Au Bučim mine and former Fe mine Damjan (Balabanova et al. 2015). An alternative approach to consider these long-term emissions (eventually more than 50 years) is to use exposed attic dust because over long periods of time atmospheric particles can accumulate within the dust, providing a record of historical local deposition (Ilacqua et al. 2003; Tye et al. 2006; Völgyesi et al. 2014). Determination of historical emissions from attic dust is based on data of the heavy metal concentrations in the attic dust from different measurement sites in terms of the weight of the total monthly air deposit (Lioy et al. 2002; Jemec Auflič and Šajn 2007; Žibret and Šajn 2008; Žibret 2008). The main idea behind determining past emissions is that heavy metal characterisation of dust deposited on a small area is multiplied by the concentration of the elements in that area and thus the mass of the pollutants which has been transported to the place of interest by air can be determined (Šajn 2006; Žibret 2008; Žibret and Šajn 2008). Undisturbed attic dust is a potential archive for atmospherically deposited particles that is known to be effective across urban areas and in the vicinity of smelters, mines, and other potential emission sources (Cizdziel et al. 1998; Cizdziel and Hodge 2000; Šajn 2000, 2001, 2002, 2003, 2005, 2006, Alijagić and Šajn 2011; Völgyesi et al. 2014; Angelovska et al. 2016). Atmospheric emissions attributed to the extraction stage of mining mainly come from wind acting on disturbed land and stockpiles of ore and waste material. As a result of these processes, dust is permanently introduced to the atmosphere (Ilacqua et al. 2003). The applicability of attic dust as a suitable long-term monitor to determine the pollution status and content in air is proven by numerous studies. Cizdziel et al. (1998) first presented respective analytical work by analysing  $^{137}\text{Cs}$  and  $^{239}\text{Pu}$  near a Nevada nuclear test site. Similar studies were conducted over the past 20 years to hunt the anthropogenic emissions sources and determine their impact on the environment (Cizdziel and Hodge 2000; Ilacqua et al. 2003; Gosar et al. 2006; Tye et al. 2006; Hensley et al. 2007; Balabanova et al. 2011; Bačeva et al. 2012; Coronas et al. 2013; Pavidonis et al. 2015). Despite the metal enrichment catchment, attic dust should be also considered as a poly-metallic marker for the lithogenic distribution of elements. De Miguel et al. (1999) proposed a dust model for tracking the natural phenomena of poly-metallic geochemical association in urban areas. However, recent investigations have focussed emphasis only on anthropogenic enrichments (Fordyce et al. 2005; Goodarzi 2006; Saeedi et al. 2012).

The present investigation was designed to determine spatially the lithogenic and anthropogenic geochemical associations in the Bregalnica River basin. This work presents a first attempt for the determination of a total of 69 elements: Ag, As, Al, Au, B, Ba, Be, Bi, Br, Ca, Cd, Ce, Co, Cr, Cs, Cu, Dy, Er, Eu, Fe, Ga, Gd, Ge, Hf, Hg, Ho, I, In, Ir, K, La, Li, Lu, Mg, Mn, Mo, Na, Nb, Nd, Ni, Os, P, Pb, Pd, Pr, Pt, Rb, Re, Rh, Ru, Sb, Sc, Se, Sm, Sn, Sr, Ta, Tb, Te, Ti, Th, Tl, Tm, V, W, Y, Yb, Zn, Zr in attic dust and topsoil samples taken from this very unique area. The appearance of dominant Oligocene volcanism in the area of the Sasa mine (Pb–Zn hydrothermal exploitation), Kratovo-Zletovo district, and Bučim mine area (Cu–Au hydrothermal exploitation) creates specific environmental conditions leading to natural and anthropogenic poly-metallic enrichments. Therefore, the main objective of this study was to assess the lithologic versus anthropogenic distribution of the mentioned elements and to extract the dominant geochemical markers correlated to air pollution and lithogenic enrichments. This way the spatial pattern of each geochemical marker will provide an overview for the health risk hotspots affected by poly-metallic deposition. This is important because of direct human exposure to these pollutants and the resulting adverse health effects.

## Investigated Area

The investigated area includes the basin of the Bregalnica River which is found in the area of the East Planning Region of the Republic of Macedonia (N  $41^{\circ}27'–42^{\circ}09'$ , E  $22^{\circ}55'–$

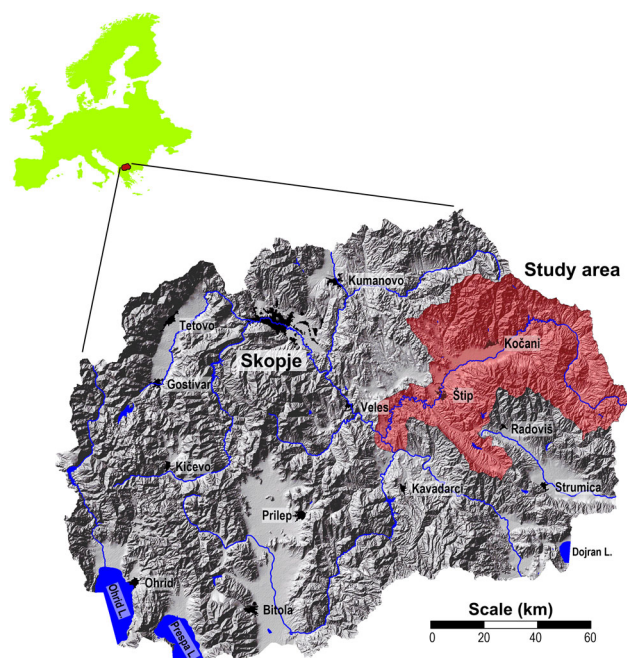


**Fig. 1** Investigated area in the territory of the Republic of Macedonia

23°01') and covers  $\sim 4000 \text{ km}^2$  (Fig. 1). The region of the investigated area is geographically composed of several sub-regions. The area is characterised by two valleys: the Maleševska and Kočani valleys. The Maleševska valley represents the upper course of the Bregalnica River where the river source also is located and has an altitude range of 700–1140 m. The valley is enclosed by the Maleševski Mountains to the east, by the Ograzhden Mountain to south-southeast, and Plačkovica and Obozna to the west. The average annual precipitation amounts to about 500 mm with significant variations from year to year, as well as in the different sub-regions (Lazarevski 1993). The precipitation is mostly related to and conditioned by the Mediterranean cyclones (Lazarevski 1993). During the summer period, the region most often is located in the centre of the subtropical anticyclone, which causes warm and dry summers. From the central area of the region, which is the driest area, the average annual precipitation increases in all directions because of the increase either in the influence of the Mediterranean climate or the increase in altitude (Lazarevski 1993). In the region about ten climatic-vegetation soil areas are distinguished with considerably heterogeneous climate, soil and vegetation characteristics (Lazarevski 1993). Regarding the demographic structure in the region of the Bregalnica basin, only 4% of the populated areas are urban areas, whereas 96% of the total populated areas are categorised as rural areas. In accordance with the data processed by the State Statistical Office (2015), the population density in the eastern region of the Republic of Macedonia is  $<51$  inhabitant on  $\text{km}^2$ . Considering land use, the region is considerably diverse. Along the course of the Bregalnica River agricultural cultivated lands dominate (Fig. 2). Pastures also are considered as agricultural lands and are represented in Fig. 2, in yellow, as open areas. Approximately 30% belong to the forest regions, localised around the Maleševska valley by the Maleševski Mountains and then around the Kočani valley by the Osogovo and Plačkovica Mountains.

### Generalised Geology of Investigated Area

The investigated area that covers the basin of the Bregalnica River lies on two main tectonic units: the Serbian-Macedonian massive and the Vardar zone (Dumurdzanov et al. 2004). The polyphasal Neogene deformations through the insignificant movements associated with the volcanic activities had a direct influence on the gradual formation of the reefs and the formation of deposits in the existing basins. From the middle Miocene to the end of the Pleistocene, there were alternating periods of fast and slow landslides accompanied with variable sedimentation (deposition). The Cenozoic volcanism represents a more recent extension in the Serbian-Macedonian massive and the Vardar zone. The

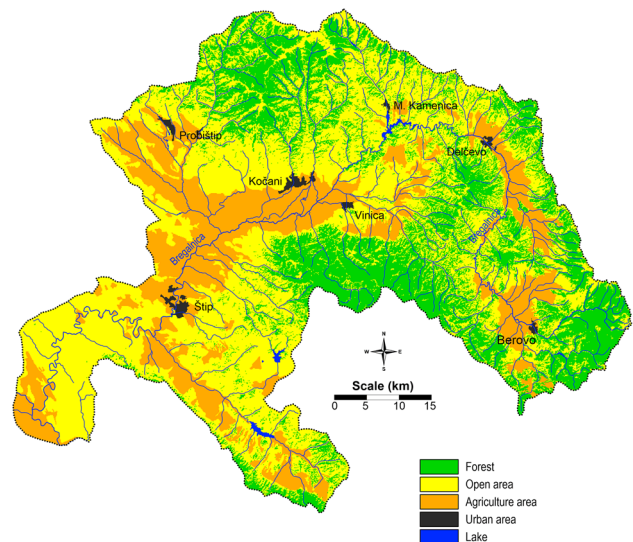


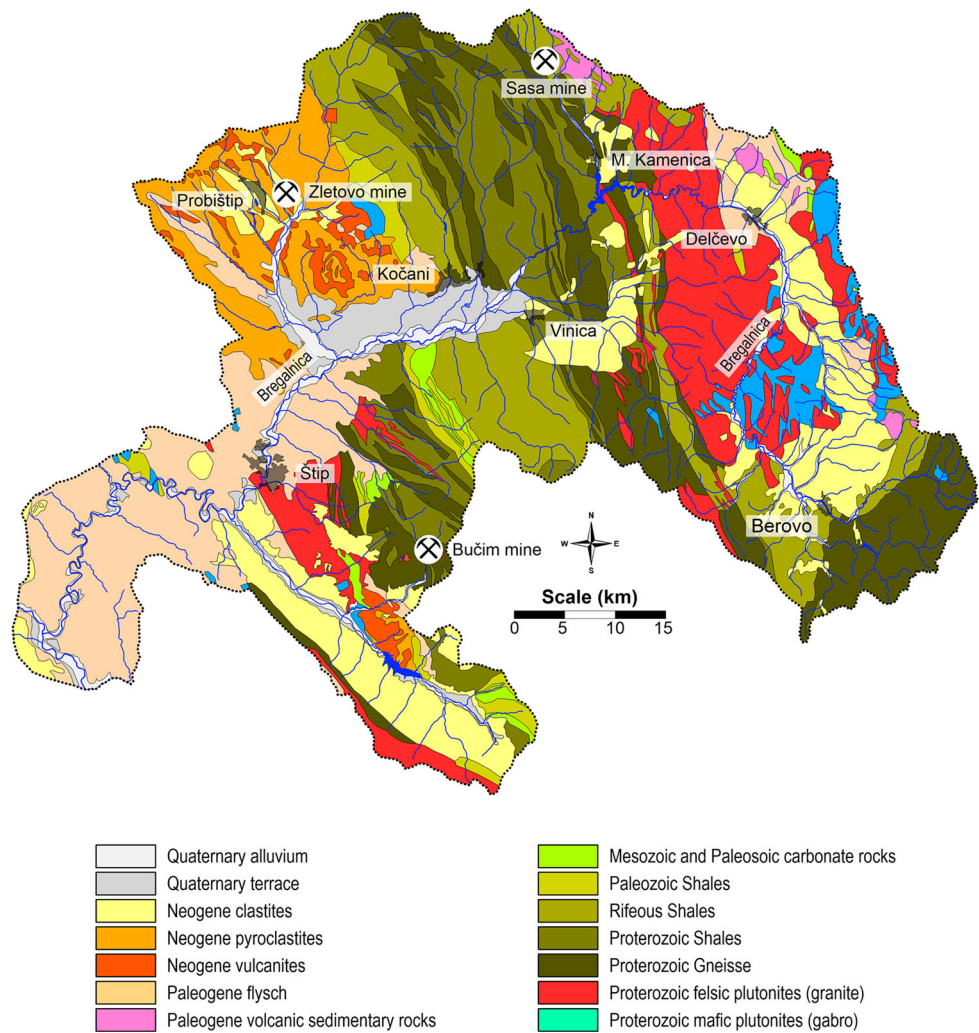
**Fig. 2** Region of the investigated area including the type of land use

oldest volcanic rocks occur in the areas of Bučim, Damjan, Borov Dol district and in the zone of Toranica, Sasa, Delčevo and Pehčevo (Dumurdzanov et al. 2004). These older volcanic rocks were formed in the mid Miocene from sedimentary rocks that represent the upper age limit of the rocks. The origin of these oldest volcanic rocks is related to the Oligocene: the early Miocene period. Volcanic rocks are categorised as follows: andesite, latite, quartz-latite, and dacite. Volcanism appears sequentially and in several phases forming subvolcanic areas. On the other hand, the pyroclastites are most frequently found in the Kratovo-Zletovo volcanic area, where the dacites and andesites are the oldest formations. Generalised geology of the area is produced based on the data provided by Rakičević et al. (1968), and the land use maps are presented in Fig. 3.

### Dominant Emission Source in the Investigated Area

The investigated area is characterised by intensive actions of hydrothermal exploitation, including: the Au–Cu mine Bučim and two Pb–Zn mines (Sasa and Zletovo). The Bučim mine and the ore processing plant were put into operation in 1979. During the flotation process of copper minerals, approximately 3950,000 tones of flotation tailings are produced annually, on average. These tailings are drained and deposited on the dump site. The dump site of the open ore pit is used for disposal of the flotation tailings brought in by dumpers. The area of the ore tailings dump site amounts to  $0.80 \text{ km}^2$ . The second emission source, the Sasa mine occupies an area of approximately  $80 \text{ km}^2$ . The mine has been in operation since 1954 and produces approximately 90,000 tones of Pb–Zn concentrate annually. Between 70,000 and  $100,000 \text{ m}^3$

**Fig. 3** Generalised geology of the whole investigated area



tailings are discharged annually, causing significant potential environmental damage (Vrhovnik et al. 2013). The continuous exploitation of the Zletovo mine began following the Second World War and has an annual production capacity of approximately 400,000 tones of Pb–Zn concentrate (9% Pb and 2% Zn) with significant participation of Ag, Bi, Cd, and Cu (Serafimovski and Tasev 2003). The ore concentration is processed through the flotation process in a plant located in the town of Probišćip, whereas the flotation tailings are left in the open in the immediate surroundings of the town.

## Materials and Methods

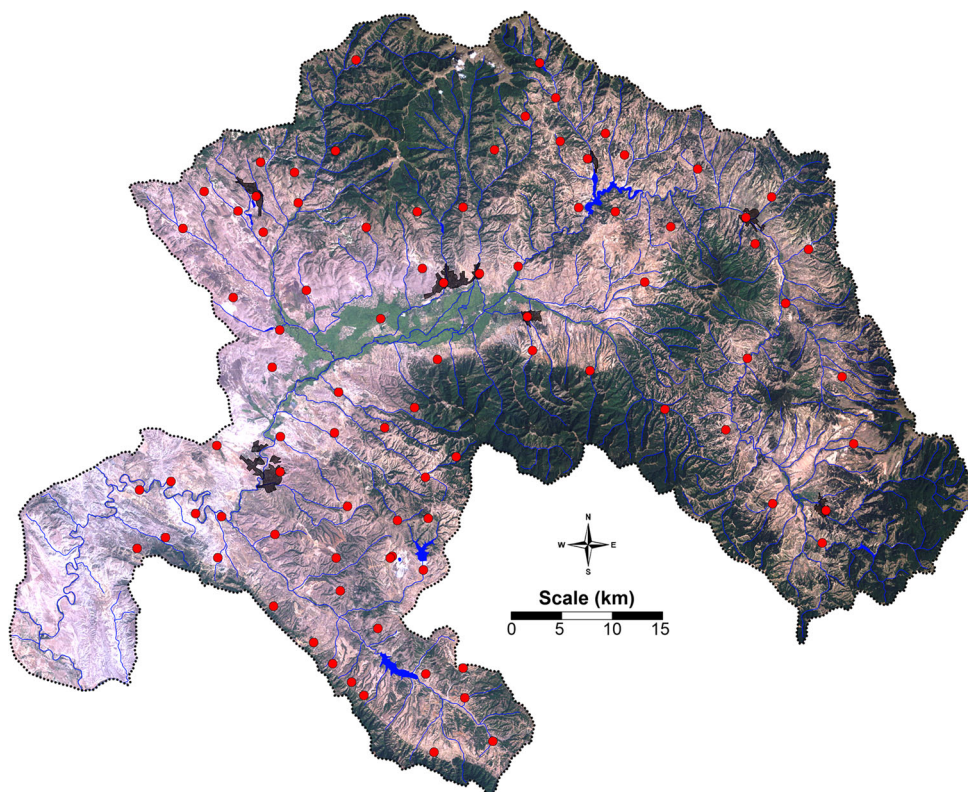
### Dataset Building Sampling Strategy

Attic dust samples were collected from the attics from total of 84 houses built between 1920 and 1970 (Fig. 4). The data information regarding the time of house construction was obtained from the local population at the time of the sampling.

The collection of attic dust samples was performed according to the protocol provided by Šajn (2003). The sampling protocol includes: (a) removing the sediments from the attic surface; (b) collecting the corpuscular dust from the attic surface using a plastic brush; and (c) transferring the collected dust in polyethylene bags. A representative sample from each house was obtained by collecting the dust from 5 to 10 attics, depending on the house condition. At each location of attic dust sampling, topsoil (0–5 cm) samples from house yards were also collected. The collecting of the samples was conducted in the period of September to November 2013.

### Sample Pretreatment

The soil samples brought to the laboratory were subjected to cleaning and homogenisation followed by drying at room temperature, or in a drying room at 40 °C, to a constant dry mass. Then the samples were passed through a 2 mm sieve and finally were homogenised by grinding in a porcelain mortar until reaching a final particle size of the particles of 125 μm.

**Fig. 4** Sampling network

Following the physical preparation, the samples were chemically prepared by wet digestion by applying a mixture of acids in accordance with the international standards (ISO 14869–1 2001).

For digestion of attic dust and soil samples, open wet digestion with a mixture of acids was applied. A precisely measured mass of dust sample (0.5 g) was placed in a Teflon vessel and 5 mL of concentrated nitric acid ( $\text{HNO}_3$ ) was added until the brown vapours were produced from the vessels. Nitric acid is a very suitable oxidant for the digestion of environmental samples. For the total digestion of inorganic components, 5–10 mL of hydrofluoric acid was added. When the digest became a clear solution, 2 mL of  $\text{HClO}_4$  was added. Perchloric acid was used for total digestion of organic matter. After 15 min of cooling the vessels, 2 mL of  $\text{HCl}$  and 5 mL of  $\text{H}_2\text{O}$  were added to the vessels to totally dissolve the metal ions. Finally, the vessels were cooled and digests quantitatively transferred to 50 mL calibrated flasks. In this way, the digested soil and sediment samples were prepared for determining the contents of the different elements using atomic emission and mass spectrometry.

#### Analytical Procedures and Quality Assurance of Measurements

A SCIEX Perkin Elmer Elan DRC II (Canada) inductively coupled plasma mass spectrometer (ICP-MS, with

quadrupole as single detector) was used for measurement of the concentration trace elements, while for the determination of major element contents determination, atomic emission with inductively coupled plasma (ICP-AES, Varian 715ES) was applied. For this study, analytical grade reagents, namely nitric acid, trace pure (Merck, Germany), hydrofluoric acid p.a. (Merck, Germany), perchloric acid p.a. (Merck, Germany), hydrochloric acid, p.a. (Merck, Germany), and redistilled water were used for preparation of all solutions. Standard solutions of metals were prepared by dilution of 1000 mg/L solutions (11355-ICP multi Element Standard). For each element analysed, previous optimisation of the instrumental conditions was performed. In all samples, the contents of a total of 69 elements were analysed: Ag, As, Al, Au, B, Ba, Be, Bi, Br, Ca, Cd, Ce, Co, Cr, Cs, Cu, Dy, Er, Eu, Fe, Ga, Gd, Ge, Hf, Hg, Ho, I, In, Ir, K, La, Li, Lu, Mg, Mn, Mo, Na, Nb, Nd, Ni, Os, P, Pb, Pd, Pr, Pt, Rb, Re, Rh, Ru, Sb, Sc, Se, Sm, Sn, Sr, Ta, Tb, Te, Ti, Th, Tl, Tm, V, W, Y, Yb, Zn, Zr. All measurements were done using the quantitative method (Total Quant) supplied by Elan 3.4 software, which uses a response factor calibration curve obtained by a calibration of multiple points, low, medium, and high mass, for optimum set-up, using a multi-element Merck VI standard solution, diluted to mimic real sample composition. The drawback is that the accuracy tends to be worse than a proper quantitative method for some elements; however,

the main advantage is that a large mass interval can be studied (up to 65 elements per each sample during a single run), which makes it a good choice for screening measurements that require a large throughput of samples with many elements of interest. For this study, a SRM 2709a (Standard reference materials, San Joaquin soil, National Institute of Standards and Technology, USA) was used to check method accuracy and for all considered elements. The calculated recovery for the certified/reference contents of the selected elements ranged from 81.3% for Sb to 113% for As (for ICP-MS measurements) and from 90.2% for Ca to 118% for Al (for ICP-AES measurements). The theoretical limit for ICP-MS methods are in ppt (ng/L) range for the majority of the elements. Matrix effects above 1 ppb ( $\mu\text{g/L}$ ) threshold while using Total Quant were not observed during our study. For some elements, values between these two levels were further investigated using more complex quantitative methods. Spiked intra-laboratory samples were analysed at a combined frequency of 20% of the samples. The recovery for all of the analysed elements ranges from 76.8% for Tl to 119% for Sb (for ICP-MS measurements) and from 87.5% for Na to 112% for P (for ICP-AES measurements).

### Data Processing and Generation of Areal Distribution Maps

The investigated elemental content data were statistically processed using statistical software (StatSoft, 11.0, Dell Software, Aliso Viejo, CA), by applying parametric and non-parametric analyses. Basic descriptive statistical analysis was conducted on elemental contents in all samples. For data normalisation, the *Box-Cox* transformation method (Box and Cox 1964) was applied within this study. Multivariate statistical methods (cluster and R-mode factor analyses) were used to reveal the associations of the chemical elements. The factor analysis was performed on variables standardised to zero mean and unit standard deviation (Šajn 2006; Žibret and Šajn 2008, 2010). For orthogonal rotation the varimax method was used. In the final multivariate factor solution, some elements were retained. The elements with low communalities were excluded because of a lack of significant associations. The universal kriging method with linear variogram interpolation was applied for the construction of spatial distribution maps of each factor score. Seven classes of the following percentile values were selected: 0–10, 10–25, 25–40, 40–60, 60–75, 75–90 and 90–100. Line and bar/colon plots were used to better visualise the element contents and trends of dust deposition according to different lithogenic units.

## Results

### Summary Results of the Data Set

Of the 69 analysed elements, values above the determined instrumental detection limits were obtained for 60 elements. Table 1 reports the descriptive statistic parameters (median and ranges values) corresponding to the content of these 60 elements in attic dust and topsoil samples from the samples attics and yards. Data filtering was conducted to upgrade this investigation. Mean values were calculated according to different lithological units in the investigated area (Table 2). The contents of the major elements in attic dust samples varied in the following ranges: Al (4–7.4%), Ca (0.58–8.6%), Fe (0.07–16%), K (0.017–4.1%), Mg (0.08–2.6%), Na (0.01–2.6%), P (0.04–0.40%), and Ti (0.002–0.79%). Almost identical results were obtained for the elements contents in topsoil samples; only for Ca and Fe were extended distribution obtained (max. value 17% and 47%, respectively).

Trace elements distribution is mainly characterised in terms of the different lithological units, as in the case of In (42  $\mu\text{g/kg}$ ), Tl (0.34 mg/kg), Bi (0.30 mg/kg), Be (0.93 mg/kg), Ho (0.46 mg/kg), Ag (0.54 mg/kg), Ge (0.57 mg/kg), and Mo (0.67 mg/kg). Tellurium distribution differs from the rest of the trace elements, due to the dominance of atmospheric deposition (with median of 31  $\mu\text{g/kg}$  and max. value of 1300  $\mu\text{g/kg}$ ) versus soil distribution (median of 17  $\mu\text{g/kg}$  and max value of 280  $\mu\text{g/kg}$ ).

Shale-normalised Rare Earth Element (REE) patterns of the Bregalnica River basin are as follow: La (18), Ce (39), Pr 4), Nd (14), Sm (2.8), Eu (0.68), Gd (3.6), Tb (0.46), Dy (2.6), Ho (0.5), Er (1.4), Tm (0.20), Yb (1.3), and Lu (0.19).

Another unique distribution was considered for the Zr and Hf atmospheric deposition. These elements range from 0.08 to 3.0 mg/kg for Hf and from 4.9 to 96 mg/kg for Zr. Enriched median values were obtained in the Paleogene and Neogene volcanics. Zirconium was enriched to 27 mg/kg for both sub-areas, while Hf was enriched to 0.68 mg/kg.

Niobium content in attic dust ranges from 0.28 to 17 mg/kg, whereas in the topsoil layer it reaches 31 mg/kg. A similar distribution was obtained for Ta: 0.05–1.3 mg/kg in attic dust and from 0.14 to 2.5 mg/kg in topsoil (Table 2).

Copper contents in the air-distributed dust ranges from 6.7 to 880 mg/kg, whereas in the topsoil layer an extended distribution occurred to 1200 mg/kg. Enriched values for the Cu content in attic dust were obtained from houses located very close to the Bučim Cu mine. Cadmium

**Table 1** Data summary for element contents in attic dust samples (D) and topsoil samples (T);  $N = 168$ 

Element	Unit	Median	Min	Max	Element	Unit	Median	Min	Max
Ag (D)	mg/kg	0.54	0.005	3.0	Mg (D)	%	0.59	0.08	2.6
Ag (T)	mg/kg	0.45	0.22	4.6	Mg (T)	%	0.47	0.06	7.2
Al (D)	%	5.7	4.0	7.4	Mn (D)	mg/kg	530	115	6900
Al (T)	%	6.0	3.0	8.9	Mn (T)	mg/kg	560	179	7000
As (D)	mg/kg	17	4.1	150	Mo (D)	mg/kg	0.67	0.005	17
As (T)	mg/kg	12	4.0	93	Mo (T)	mg/kg	0.48	0.005	8.3
B (D)	mg/kg	11	0.005	63	Na (D)	%	0.48	0.01	2.6
B (T)	mg/kg	0.56	0.005	42	Na (T)	%	0.78	0.08	3.3
Ba (D)	mg/kg	400	6.8	1400	Nb (D)	mg/kg	5.8	0.28	17
Ba (T)	mg/kg	420	76	2600	Nb (T)	mg/kg	5.8	2.4	31
Be (D)	mg/kg	0.93	0.13	3.4	Nd (D)	mg/kg	13	0.37	42
Be (T)	mg/kg	1.1	0.12	4.6	Nd (T)	mg/kg	12	3.1	69
Bi (D)	mg/kg	0.30	0.005	5.9	Ni (D)	mg/kg	21	4.4	250
Bi (T)	mg/kg	0.19	0.046	1.6	Ni (T)	mg/kg	14	4.6	260
Br (D)	mg/kg	2.4	0.005	20	P (D)	%	0.21	0.04	0.40
Br (T)	mg/kg	1.6	0.005	15	P (T)	%	0.07	0.01	0.31
Ca (D)	%	3.9	0.58	8.6	Pb (D)	mg/kg	51	0.005	3900
Ca (T)	%	2.3	0.26	17	Pb (T)	mg/kg	22	0.005	1200
Cd (D)	mg/kg	0.43	0.054	25	Pd (D)	mg/kg	0.35	0.05	1.4
Cd (T)	mg/kg	0.13	0.005	9.0	Pd (T)	mg/kg	0.31	0.05	1.7
Ce (D)	mg/kg	39	0.80	130	Pr (D)	mg/kg	3.6	0.08	11
Ce (T)	mg/kg	36	8.2	160	Pr (T)	mg/kg	3.5	0.82	18
Co (D)	mg/kg	6.6	0.94	20	Pt (D)	mg/kg	0.21	0.005	0.81
Co (T)	mg/kg	6.7	2.5	47	Pt (T)	mg/kg	0.16	0.005	0.78
Cr (D)	mg/kg	48	11	270	Rb (D)	mg/kg	48	3.5	120
Cr (T)	mg/kg	38	3.8	330	Rb (T)	mg/kg	54	9.2	250
Cs (D)	mg/kg	2.3	0.005	12	Sb (D)	mg/kg	0.63	0.060	3.2
Cs (T)	mg/kg	2.6	0.35	27	Sb (T)	mg/kg	0.42	0.10	3.9
Cu (D)	mg/kg	30	6.7	880	Sc (D)	mg/kg	6.9	0.54	92
Cu (T)	mg/kg	17	4.1	1200	Sc (T)	mg/kg	6.2	1.1	26
Dy (D)	mg/kg	2.5	0.08	7.8	Sm (D)	mg/kg	2.8	0.05	8.0
Dy (T)	mg/kg	2.3	0.66	15	Sm (T)	mg/kg	2.5	0.65	14
Er (D)	mg/kg	1.3	0.03	4.0	Sn (D)	mg/kg	3.2	0.005	23
Er (T)	mg/kg	1.2	0.35	7.6	Sn (T)	mg/kg	1.5	0.005	14
Eu (D)	mg/kg	0.72	0.02	2.3	Sr (D)	mg/kg	140	6.0	720
Eu (T)	mg/kg	0.68	0.16	4.7	Sr (T)	mg/kg	110	23	760
Fe (D)	%	1.5	0.07	16	Ta (D)	mg/kg	0.46	0.05	1.3
Fe (T)	%	1.5	0.18	47	Ta (T)	mg/kg	0.54	0.14	2.5
Ga (D)	mg/kg	9.1	2.1	20	Tb(D)	mg/kg	0.47	0.02	1.3
Ga (T)	mg/kg	9.2	5.3	56	Tb (T)	mg/kg	0.43	0.12	2.7
Gd (D)	mg/kg	3.6	0.13	10	Te (D)	μg/kg	31	5.0	1300
Gd (T)	mg/kg	3.3	0.95	21	Te (T)	μg/kg	17	5.0	280
Ge (D)	mg/kg	0.57	0.27	2.1	Ti (D)	%	0.23	0.002	0.79
Ge (T)	mg/kg	0.62	0.40	2.6	Ti (T)	%	0.22	0.03	0.96
Hf (D)	mg/kg	0.63	0.02	1.9	Tl (D)	mg/kg	0.34	0.05	1.7
Hf (T)	mg/kg	0.56	0.08	3.0	Tl (T)	mg/kg	0.38	0.05	2.5
Ho (D)	mg/kg	0.46	0.01	1.5	Tm (D)	mg/kg	0.18	0.01	0.52
Ho (T)	mg/kg	0.43	0.12	2.8	Tm (T)	mg/kg	0.17	0.05	1.1

**Table 1** continued

Element	Unit	Median	Min	Max	Element	Unit	Median	Min	Max
I (D)	mg/kg	0.14	0.005	0.53	V (D)	mg/kg	72	29	370
I (T)	mg/kg	0.11	0.02	0.71	V (T)	mg/kg	62	28	600
In (D)	µg/kg	42	5.0	710	W (D)	mg/kg	1.0	0.045	8.9
In (T)	µg/kg	31	11	190	W (T)	mg/kg	0.99	0.24	5.9
K (D)	%	0.83	0.017	4.1	Y (D)	mg/kg	11	0.44	30
K (T)	%	0.89	0.16	6.1	Y (T)	mg/kg	8.9	2.4	58
La (D)	mg/kg	18	0.37	52	Yb (D)	mg/kg	1.1	0.050	3.4
La (T)	mg/kg	16	3.6	72	Yb (T)	mg/kg	1.1	0.33	7.1
Li (D)	mg/kg	13	3.4	44	Zn (D)	mg/kg	99	26	3200
Li (T)	mg/kg	13	2.8	65	Zn (T)	mg/kg	53	18	590
Lu (D)	mg/kg	0.17	0.005	0.56	Zr (D)	mg/kg	24	0.42	61
Lu (T)	mg/kg	0.17	0.05	1.1	Zr (T)	mg/kg	21	4.9	96

contents also showed an enrichment trend in air-distributed dust (0.054–25 mg/kg); however, Cd content in the topsoil layer did not indicate any significant enrichment (0.005–9 mg/kg). The distribution of Pb and Zn is similar to that of Cu and Cd in the investigated area. Lead content ranges from 0.005 to 3900 mg/kg, while Zn contents show lower enrichments from 26 to 3200 mg/kg. Lithogenic distribution in soil reaches to 1200 mg/kg and 590 mg/kg, for Pb and Zn, respectively. According to the dominant lithological units, Rifeous shales are mostly enriched with Pb and Zn, where the median values for Pb and Zn contents are 110 and 220 mg/kg, respectively.

From the platinum group, Pt and Pd were determined in traces above the instrumental detection limit. Their content distributions are almost identical in attic dust and in surface soil. Platinum ranges from 0.005 to 0.78 mg/kg in soil, while in dust it reaches to 0.81 mg/kg. Palladium is the more dominant platinum element, and ranges from 0.05 to 1.4 mg/kg in attic dust and reaches 1.7 mg/kg in soil (Table 2).

### Multivariate Assessment of the Dominant Geochemical Markers

Multivariate extraction was applied to reduce the numerous element distributions and to identify the dominant geochemical associations. On the basis of the matrix of correlation coefficients, multivariate cluster and R-mode factor analysis was used to reveal associations of chemical elements and to decrease the number of variables for the obtained data. Extraction was simplified to six factor associations, marked as: F1: Ga–Nb–Ta–Y–(La–Gd)–(Eu–Lu), F2: Be–Cr–Li–Mg–Ni; F3: Ag–Bi–Cd–Cu–In–Mn–Pb–Sb–Te–W–Zn, F4: Ba–Cs–Hf–Pd–Rb–Sr–Tl–Zr; F5: As–Co–Ge–V, F6: K–Na–Sc–Ti, accounting for a total variability for dominant loadings of 81.5%. Table 3

summarises the factor loadings for dominant element associations. It was assumed that variables with factor loadings greater than 0.5 significantly contribute significantly to any particular factor. The remaining elements were eliminated from the analysis, due to their tendency to form separate clusters, thus not showing a reasonable connection with other chemical elements and to satisfy the criteria of the dimension variables based on the number of observations. Elements with a low share of communality or tendency to form independent factors were also excluded. Factor analysis (FA) was performed on elements standardised to zero mean and unit standard deviation. The inter-element similarity and distancing were revealed using a cluster dendrogram (Fig. 5). The most distant clusters were Factor 1 [Ga–Nb–Ta–Y–(La–Gd)–(Eu–Lu)] and Factor 3 (Ag–Bi–Cd–Cu–In–Mn–Pb–Sb–Te–W–Zn).

### Areal Distribution Mapping of the Factors

Factors patterns were characterised according to dominant lithological units to determine the basic geochemical markers in the investigated area (Figs. 6, 7, 8, 9, 10, 11, 12, and 13). Bar plots were created, to reveal the impact of dominant geological units on geochemistry of the elemental associations. Dominant lithological units were singled out as: the Quaternary alluvial (along the whole course of Bregalnica River) and terraces, Neogene sediment and pyroclastite (dominant volcanic rocks from the Kratovo-Zletovo district), Paleogene flysch, Rifeous schist, Proterozoic schist, gneiss and granites. Figure 6 summarises the distribution of extracted factor associations according to the dominant lithological units.

For the spatial distribution of the factor scores, universal kriging with a linear variogram interpolation method (Beelen et al. 2009) was applied for the construction of



**Table 2** Element distribution according to dominant geological formation in the area (median values are given,  $N = 84$ )

Element	Unit	River terraces (Q)	River sediment (Ng)	Pyroclastite (Ng)	Flysh (Pg)	Schists (Pz)	Schists (R)	Schists (Pt)	Gneisses (Pt)	Granite (Pt)
Ag	mg/kg	0.53	0.48	0.59	0.45	0.60	1.3	0.44	0.43	0.58
Al	%	5.2	5.3	5.9	5.5	5.8	5.1	5.8	6.0	5.5
As	mg/kg	19	23	16	21	16	26	20	15	14
B	mg/kg	8.8	9.7	7.4	6.3	9.5	4.9	12	5.8	4.7
Ba	mg/kg	330	330	500	400	370	340	370	310	470
Be	mg/kg	0.91	1.2	0.89	0.77	1.1	0.77	0.98	0.81	0.68
Bi	mg/kg	0.28	0.28	0.31	0.29	0.26	0.61	0.45	0.35	0.22
Br	mg/kg	5.3	2.7	2.3	1.9	2.2	2.9	2.1	2.0	1.1
Ca	%	5.0	3.7	3.9	5.1	3.7	4.9	4.0	3.4	4.1
Cd	mg/kg	0.42	0.45	0.44	0.52	0.33	1.5	0.28	0.25	0.31
Ce	mg/kg	28	22	41	33	35	36	39	42	38
Co	mg/kg	6.6	5.6	7.2	6.0	7.3	9.1	6.4	6.5	7.6
Cr	mg/kg	48	30	42	34	59	50	43	39	47
Cs	mg/kg	2.2	1.6	3.0	3.3	2.2	2.4	2.1	1.7	1.7
Cu	mg/kg	40	25	27	24	25	43	49	26	29
Dy	mg/kg	1.9	1.8	2.4	2.0	2.6	2.3	2.4	3.3	2.6
Er	mg/kg	0.98	0.91	1.2	1.0	1.4	1.2	1.2	1.7	1.3
Eu	mg/kg	0.58	0.60	0.77	0.63	0.68	0.67	0.68	0.82	0.77
Fe	%	1.4	1.3	0.95	1.3	1.4	1.2	1.1	1.1	1.6
Ga	mg/kg	7.1	7.1	9.4	7.6	9.9	10	8.9	9.0	8.5
Gd	mg/kg	2.8	2.7	3.6	2.9	3.6	3.3	3.6	4.6	3.8
Ge	mg/kg	0.53	0.51	0.60	0.55	0.65	0.75	0.64	0.52	0.52
Hf	mg/kg	0.52	0.45	0.68	0.64	0.59	0.47	0.46	0.60	0.62
Ho	mg/kg	0.36	0.32	0.46	0.37	0.50	0.43	0.44	0.62	0.49
I	mg/kg	0.15	0.10	0.15	0.17	0.15	0.12	0.11	0.11	0.12
In	µg/kg	35	28	46	37	42	94	46	34	39
K	%	0.86	1.0	0.94	0.79	0.95	0.73	0.70	0.70	0.78
La	mg/kg	13	11	19	15	15	17	18	19	18
Li	mg/kg	16	12	12	10	14	10	11	10	9.3
Lu	mg/kg	0.15	0.14	0.18	0.15	0.19	0.16	0.17	0.21	0.18
Mg	%	0.62	0.62	0.51	0.41	0.77	0.44	0.56	0.53	0.40
Mn	mg/kg	440	450	540	480	560	830	530	370	430
Mo	mg/kg	0.10	0.72	0.23	0.25	0.26	0.70	1.3	0.65	0.79
Na	%	0.47	0.68	0.45	0.39	0.62	0.39	0.38	0.54	0.46
Nb	mg/kg	4.9	4.5	6.2	5.3	6.8	5.4	6.8	6.9	6.0
Nd	mg/kg	9.8	8.9	14	11	13	12	14	16	14
Ni	mg/kg	19	14	23	17	25	23	23	15	16
P	%	0.22	0.23	0.21	0.26	0.17	0.21	0.19	0.19	0.20
Pb	mg/kg	54	83	48	18	30	110	55	22	12
Pd	mg/kg	0.35	0.35	0.35	0.44	0.33	0.30	0.25	0.28	0.38
Pr	mg/kg	2.5	2.3	3.8	3.0	3.4	3.1	4.0	4.0	3.4
Pt	mg/kg	0.22	0.20	0.20	0.20	0.18	0.23	0.15	0.22	0.20
Rb	mg/kg	43	36	54	47	53	54	47	40	37
Sb	mg/kg	0.80	0.64	0.89	0.62	0.55	1.1	0.66	0.45	0.46
Sc	mg/kg	6.0	5.1	9.6	5.7	6.7	5.8	5.1	7.7	7.9
Sm	mg/kg	2.0	1.8	2.8	2.2	2.7	2.5	2.8	3.4	2.9
Sn	mg/kg	2.8	2.2	2.9	2.4	2.5	4.6	2.9	3.4	3.5
Sr	mg/kg	130	110	190	160	160	130	130	100	110

**Table 2** continued

Element	Unit	River terraces (Q)	River sediment (Ng)	Pyroclastite (Ng)	Flysh (Pg)	Schists (Pz)	Schists (R)	Schists (Pt)	Gneisses (Pt)	Granite (Pt)
Ta	mg/kg	0.33	0.34	0.46	0.38	0.50	0.37	0.47	0.56	0.48
Tb	mg/kg	0.36	0.34	0.46	0.38	0.48	0.44	0.46	0.61	0.50
Te	µg/kg	34	15	30	27	28	63	41	21	19
Ti	%	0.22	0.20	0.25	0.20	0.26	0.18	0.25	0.32	0.25
Tl	mg/kg	0.27	0.29	0.40	0.40	0.33	0.38	0.40	0.25	0.25
Tm	mg/kg	0.14	0.13	0.18	0.15	0.20	0.16	0.17	0.23	0.18
V	mg/kg	68	100	79	68	74	75	87	76	71
W	mg/kg	0.85	0.79	1.0	0.76	1.0	2.0	1.1	1.1	0.76
Y	mg/kg	9.2	7.4	11	8.5	12	11	11	13	11
Yb	mg/kg	0.93	0.87	1.2	0.96	1.3	1.1	1.1	1.5	1.2
Zn	mg/kg	110	130	98	110	90	220	86	72	88
Zr	mg/kg	23	18	27	27	23	20	20	22	23

Q quaternary, Ng Neogene, Pg Paleogene, R Rifey, Pt Proterozoic, Pz Paleozoic

maps showing the spatial distribution of factor scores (F1–F6). The significance is provided on those areas where the content of the element exceeds the 75th percentile of the data distribution for the element content.

## Discussion

### Single Element Distribution Versus Geochemistry of Their Occurrence

Enrichments of major elements (Al, Ca, Fe, K, Mg, Na, P, and Ti) in Paleogene flysch areas suggest deposition during an early stage of orogenesis. The natural abundance of the major elements is strongly correlated to the sedimentary rocks in the investigated area. Keller et al. (2015) observed similar anomalous composition rarity while investigating the volcanic-plutonic parity. Enrichments in volcanic Ti and K also may suggest the influence of peralkaline volcanics on the geochemistry of these elements. The distribution of the major elements in the air distributed dust is affected by the soil surface wind-blow dusting. The investigated area present a unique area of interweaves of the widely distributed rocks types formed by high-grade regional metamorphic processes. More dynamic differences between lithogenic distributions in soil versus elemental dust deposition occur for trace elements.

Trace element abundances consistently diverge in zones where different lithological units occur. rubidium, Cs, Sr, and Ba, often are collectively termed the large-ion-lithophile (LIL) elements. Due to their solubility, they are quite mobile during metamorphism and weathering. Thus, the factors that most strongly govern their behaviour in igneous rocks are ionic radius and charge. Their

enrichment in the investigated area was also correlated with intensive depositions in subareas where the occurrence of Neogene pyroclastite dominates (Table 2). In contrast to the heavy alkaline earths metals, Be and Li show some different trends in chalcophile/lithophile deposition. River sediments are predominantly where the maximum contents of Be and Li were deposited (3.4 and 44 mg/kg, respectively).

Characterisation of REE distribution in automorphic and alluvial soil, reveals that the sum for total light rare earth elements ( $\Sigma$ LREEs) in the Bregalnica River basin ranges from 8.6 to 225 mg/kg, whereas for the total sum of the heavy rare earth elements ( $\Sigma$ HREEs) ranges from 0.92 to 33.7 mg/kg (Balabanova et al. 2015).

Like the alkalis and alkaline earths, the REEs and Y are strongly electropositive; thus, they have very similar geochemistry in the environment. Their abundance is usually correlated to many continental rocks, as well as most sediment. Many sedimentary rocks and seawater (as suggested by Wong et al. 2006) have similar REE patterns, which are similar to each other and to that of the continental crust. To accentuate the difference in REE patterns between sediments, low temperature geochemists often normalise REE abundances to the concentrations in average shale. As the REEs are highly insoluble and immobile, REE patterns often remain unchanged during metamorphism (Jemec Aulfič and Šajn 2007). Hence, REE patterns can provide information on the premetamorphic history of a rock. Indeed, even during the production of sediment from crystalline rock, the REE patterns often remain little changed and can be used to identify the provenance (i.e., the source) of sedimentary rocks.

Zirconium and Hf are nominally incompatible with all major rock-forming minerals. Keller et al. (2015)

**Table 3** Matrix of factor loadings-factor analysis (FA) of the element contents in samples

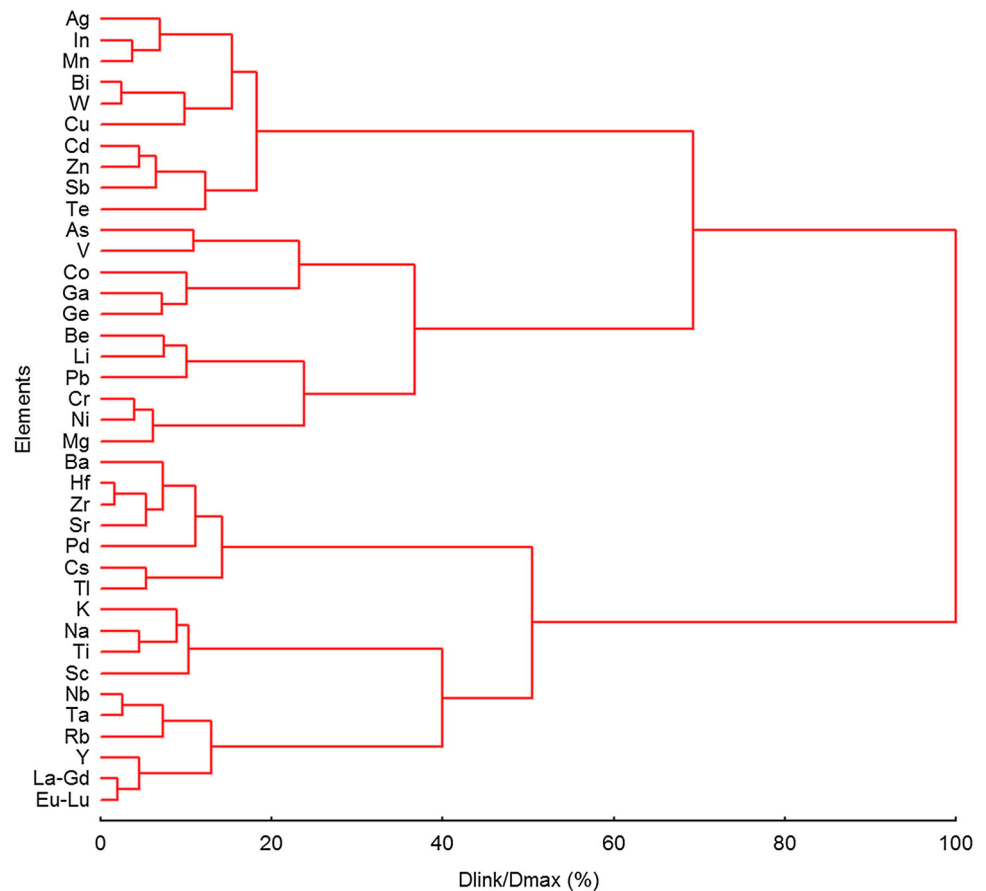
Element	F1	F2	F3	F4	F5	F6	Communality
Ga	<b>0.64</b>	0.15	0.06	0.29	<b>0.59</b>	0.16	89.9
Nb	<b>0.80</b>	0.17	0.18	0.22	−0.02	0.27	82.8
Ta	<b>0.77</b>	0.07	0.16	0.42	−0.08	0.19	84.5
Y	<b>0.87</b>	0.17	0.14	0.11	0.00	0.21	86.4
La–Gd	<b>0.81</b>	−0.02	0.12	<b>0.51</b>	0.00	0.04	92.8
Eu–Lu	<b>0.79</b>	0.03	0.11	0.40	0.04	0.19	83.6
Be	0.11	<b>0.53</b>	0.41	0.10	0.25	0.42	71.1
Cr	0.24	<b>0.83</b>	−0.06	−0.10	0.23	0.20	85.4
Li	−0.06	<b>0.76</b>	0.22	0.33	0.10	0.18	77.8
Mg	0.10	<b>0.84</b>	0.17	−0.13	0.06	0.37	90.5
Ni	0.09	<b>0.89</b>	0.09	0.05	0.11	0.00	82.7
Ag	0.31	0.05	<b>0.73</b>	0.13	0.23	0.10	71.1
Bi	0.23	0.01	<b>0.88</b>	0.09	−0.09	0.03	84.7
Cd	−0.06	−0.01	<b>0.82</b>	0.36	0.08	0.08	81.6
Cu	0.26	0.32	<b>0.64</b>	−0.06	0.08	0.20	63.7
In	0.40	−0.18	<b>0.70</b>	0.31	0.21	0.08	82.8
Mn	0.27	0.20	<b>0.68</b>	0.31	0.35	0.21	83.3
Pb	−0.11	0.35	<b>0.77</b>	−0.05	−0.13	0.24	80.6
Sb	−0.13	0.16	<b>0.77</b>	0.38	0.00	0.14	79.9
Te	0.02	0.23	<b>0.73</b>	0.04	0.31	−0.13	70.2
W	0.38	0.08	<b>0.85</b>	0.20	−0.01	0.01	90.7
Zn	−0.11	−0.03	<b>0.74</b>	0.18	0.30	0.24	74.36
Ba	0.38	−0.26	0.05	<b>0.79</b>	0.00	0.10	84.2
Cs	0.20	0.21	0.31	<b>0.76</b>	−0.22	−0.17	83.9
Hf	0.34	0.00	0.12	<b>0.86</b>	0.01	0.14	87.9
Pd	0.05	−0.04	0.03	<b>0.73</b>	0.43	0.22	78.4
Rb	<b>0.51</b>	0.25	0.29	<b>0.55</b>	0.02	0.04	71.3
Sr	0.17	0.10	0.31	<b>0.82</b>	0.11	0.16	84.1
Tl	0.22	−0.03	<b>0.51</b>	<b>0.72</b>	−0.01	−0.08	83.9
Zr	0.30	0.12	0.15	<b>0.84</b>	0.07	0.16	86.9
As	−0.42	0.11	0.33	0.02	<b>0.72</b>	−0.15	83.5
Co	0.35	<b>0.44</b>	0.28	0.23	<b>0.45</b>	0.31	74.1
Ge	0.18	0.29	0.19	0.04	<b>0.86</b>	0.06	89.8
V	−0.23	0.30	0.10	−0.13	<b>0.59</b>	<b>0.53</b>	80.2
K	0.08	0.31	0.30	0.38	0.11	<b>0.67</b>	80.2
Na	0.28	0.18	0.11	0.10	0.15	<b>0.84</b>	85.9
Sc	0.29	0.14	0.11	0.19	−0.06	<b>0.69</b>	63.8
Ti	<b>0.50</b>	0.21	0.10	0.03	−0.03	<b>0.76</b>	88.7
Total variability (%)	15.6	11.3	20.1	16.8	8.03	9.61	<b>81.5</b>
Eigene value	15.2	5.36	4.36	2.46	1.91	1.71	

F1, F2, F3, F4, F5 and F6 factor loadings. Dominant values are bolded

reported that the decreasing trends of Zr and Hf with increasing silica reflected the saturation of zircon ( $\text{ZrSiO}_4$ ). Rubatto (2002) and Kabata-Pendias (2010) observed that these elements tend to be very immobile during weathering and metamorphism. They are therefore particularly valuable in the study of ancient igneous rock suites, because they can sometimes

provide insights into the environment in which those rocks formed.

Tantalum Nb are present in anomalously low concentrations in magmas associated with subduction zones; indeed, this is considered a diagnostic feature of subduction-related volcanism (Keller et al. 2015). Although this depletion is not well understood, it is probably at least in

**Fig. 5** Dendrogram of the dominant clusters

part a consequence of the low solubility of these elements and the consequent failure of aqueous fluids generated by dehydration of the subducting oceanic crust to transport these elements into the magma genesis zone (Keller et al. 2015).

The lithogenic abundance of the platinum group (as mentioned in the Results section for Pt and Pd) along the Bregalnica River basin stays very constant, with no significant variations versus dominant lithogenic units. White (2013) reported that chromites and sulfides are highly enriched in noble metals relative to silicate magmatic rocks, consistent with their chalcophile nature and demonstrated affinity for oxide phases such as the spinels. Their dominance increased in the area where the Paleogene flysch and Rifeous schists are the dominant lithogenic units.

The geochemistry of the transition elements is considerably more complex than that of the elements we have discussed thus far. Stafilov et al. (2012) reported the anthropogenic anomaly of Cu deposition in Cd, Cr, Cu, Ni, Pb, and Zn mines environments (max values: 3.1, 110, 415, 59, 121, and 93 mg/kg, respectively). Stafilov et al. (2010) and Balabanova et al. (2012) also explained that urban elements and those related to mine activities in dust were associated with fine particles, which are preferentially

mobilised by wind and trapped in attics. The present investigation also demonstrates a very similar anomaly for the above-mentioned elements. The basic *hotspots* singled out in the environment very close to Bučim (for Cu distribution predominantly), Sasa mine and Zletovo mine. The significant enrichments of Cd, Cu, Pb, and Zn that occurred in the deposited air distributed dust have no correlation with the surface soil inputs. Therefore, the attic dust depositions indicate that on long time scale anthropogenic activities affected the distribution of elements in mine environments. For the deposition of Cd and Cu, despite hydrothermal exploitation activity, sources with different origin can affect on their enrichments in environment. For example, Bourennane et al. (2010) reported that Cd enrichments of topsoil horizons is ascribed to agricultural activities, such as the use of urban sludge, manure, and phosphate-enriched fertilisers that are known to contain Cd in addition to atmospheric deposition. On the other hand, the significantly enriched contents of Pb and Zn are due to the wind blowing dusting the soil surface layer in areas where Rifeous shales occurrence is dominant. The Sasa mine environment is the area most affected by Pb/Zn enrichment due to the continually long-term wind dust dispersion from the flotation tailings.

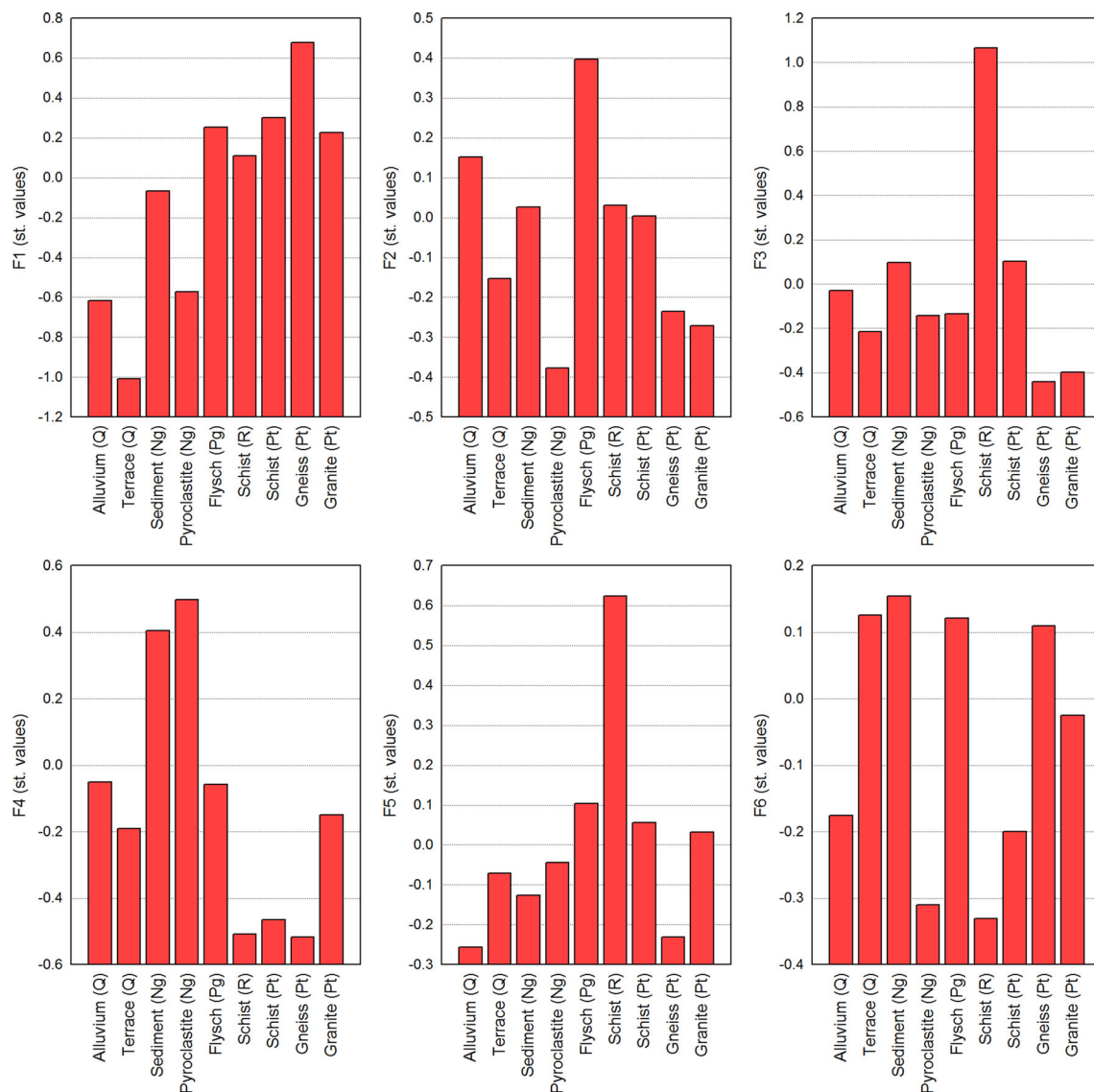


**Fig. 6** Distribution of elements associations according to dominant geological units (*Q* quaternary; *Ng* Neogene; *Pg* Paleogene; *R* Rifej; *Pt* Proterozoic)

### Enchasing the Dominant Geochemical Markers

Distribution of Factor 1 [Ga–Nb–Ta–Y–(La–Gd)–(Eu–Lu)] clearly expresses the typical connection of some basic earth forming process, due to the incorporation of the REE. Their sources are mainly natural phenomena such as rock weathering and chemical processes in the soil. White (2013) explained that many sedimentary rocks have similar REE patterns that are similar to each other, and to that of the continental crust. However, the geochemistry of the REE in the investigated area does not dominate in the sedimentary rocks. Occurrence of this factor is typical for the Proterozoic formations (gneisses, granites, and shale; Fig. 6). As the REE are highly insoluble and immobile, REE patterns often remain unchanged during

metamorphism. Hence, REE patterns can provide information on the premetamorphic history of a rock. Indeed, even during the production of sediment from crystalline rock, the REE patterns often remain little changed and are therefore used to identify the provenance (i.e., the source) of sedimentary rocks. A unique occurrence is correlation of these elements with Ta and Nb. These elements are present in anomalously low concentrations in magmas associated with subduction zones (this is considered a diagnostic feature of subduction-related volcanism). Figure 7 visualises the maximum patterns for elements deposition: proterozoic gneisses were most dominant in areas with F1 enrichments.

The second geochemical association (Be–Cr–Li–Mg–Ni) also is related to the effects of windblown dust from the

surface soil layers (Fig. 8). These elements are considered “natural,” because their origin is primarily crustal-soil particles suspended and transported by wind. High factor loadings are related to some old formation, such as Paleogene flysch and Quaternary unconsolidated sediments (Fig. 6). The enriched content of Cr-Ni in different environmental samples along the Vardar zone is repeatedly demonstrated in Macedonia (Stafilov et al. 2010; Popov et al. 2014; Barandovski et al. 2015) and in Balkan countries (Salminen et al. 2005). Higher contents of the aforementioned elements is found in dust distributed along the valleys of the Vardar and Crna rivers, where a constant flow of air masses is present in both direction (Lazarevski 1993), indicating the influence of the lithological background (Bačeva et al. 2012). The specific distribution of Be-Cr-Li-Mg-Ni extended in a SE direction in the vicinity of the town of Berovo. There are data that suggest a poly-metallic enrichment in this area (Arsovski 1997). These elements also can be connected to air pollution. Most emissions of these elements to the environment originate from local sources, mainly from mines and smelters (Stafilov 2014). Furthermore, this association can be used for the identification of the poly-metallic anomalies as a secondary occurrence.

Factor 3 (Ag-Bi-Cd-Cu-In-Mn-Pb-Sb-Te-W-Zn) was the most heterogenic geochemical association. Enriched deposition occurred predominantly on Rifeous shale (Fig. 6). These very old rocks occur as transition lithologic units between the Neogene and Paleogene volcanism in the study area. The Pb-Zn Sasa and Zletovo mines are located in the areas where Oligocene and Neogene volcanism appears sequentially and in several phases, forming sub-volcanic areas. On the other hand, the pyroclastites are most frequently found in the Kratovo-Zletovo volcanic area, where the dacites and andesites are the oldest formations. This geochemical association links elements that are normally associated with air pollution (Cd-Pb-Zn) and usually are not influenced by lithological background (Fig. 9). Spatial patterns show intensive deposition in the area of poly-metallic hydrothermal exploitations (i.e., Sasa, Zletovo, and Bučim) (Fig. 9). Thus, this factor can explain and mark the anthropogenic affects on air pollution. These anthropogenic anomalies have a historical record, several long, of continuously introducing significant dust particle emissions of dust particle with enriched contents of Cd, Pb, and Zn (Fig. 10). Also, this investigation fortifies an extended anthropogenic association (Ag, Bi, In, and Mn) that involves some other anthropogenic activities such as agricultural activities (use of urban sludge, manure, and phosphate fertilisers) or their occurrence can be a secondary affection from mine poly-metallic pollution (Stafilov et al. 2010; Ajmone-Marsan et al. 2008; Barandovski et al. 2015). Affiliation of Te and W to this

group produced a novel poly-metallic/metalloid anomaly in the Berovo region. For all elements that associate in this group, enriched deposition values are in this area. Almost 20 years ago, Arsovski (1997) drew attention to poly-metallic enrichment in this area (so-called Vladimirovo-Berovo), during the tectonic investigation. The present investigation also finds interpolates this area to be a metallic-/metalloids enriched zone, with emphasis on the anthropogenic elements.

The occurrence of Factor 4 (Ba-Cs-Sr-Rb-Pd-Tl-Zr-Hf), presents an interesting geochemical association, which incorporates the incompatible/hygro-magmatophile elements (Fig. 11). Element enrichments occur in areas where Neogene pyroclastite and sediments are dominant (Fig. 6). According to the generalised geology map (Fig. 3), the Kratovo-Zletovo region is a unique district in the region located along the continental margin and is closely related to the Tertiary volcanoes and hydrothermal activities in this area. According to Dumurdzanov et al. (2004) the pyroclastites are most frequently found in the Kratovo-Zletovo volcanic area, where the dacites and andesites are the oldest formations. These polyphasal Neogene deformations, through insignificant movements associated with the volcanic activities had a direct influence on the gradual formation of the reefs and the formation of deposits in the Zletovo area. Spatial patterns are extended in an eastern direction due to the most common winds direction being from the west with a frequency of 19.9% and speed of 2.7 m/s (Lazarevski 1993). Barandovski et al. (2015) singled out lithogenic markers of Ba-Cs association enriched in areas of felsic volcanic rocks (andesite) and found that their pyroclastic rocks primarily occupy the Kriva Reka basin, bordered by the Kratovo-Zletovo region. The same geochemical anomaly occurs in smaller zones (Kožuf and Mariovo regions).

Factor 5 associates the following elements, As, Co, Ge, and V, with the predominant occurrence on Rifeous shales (Fig. 6). This kind of geochemical *fingerprinting* occurs along the whole course of the Bregalnica River. Accordingly, the resulting areal distribution map is used to support with high certainty the assessment for poly-metallic enrichments ascribed to urbanisation, including vehicular emissions and incinerators and industry. Comparative analysis of the areal patterns identified very similar behaviour of Factors 3 and 5. The clustering method was very useful for determining both geochemical associations. The dendrogram displays a very close interpolation of the aforementioned elements from F3 and F5. Furthermore, there is a strong interconnection between the anthropogenic and lithogenic fingerprinting, which is, essentially, the element geochemistry intermediate between atmospheric emissions and lithogenic wind-blown dust. Therefore, the

**Fig. 7** Distribution patterns for *Factor 1* Ga–Nb–Ta–Y–(La–Gd)–(Eu–Lu)

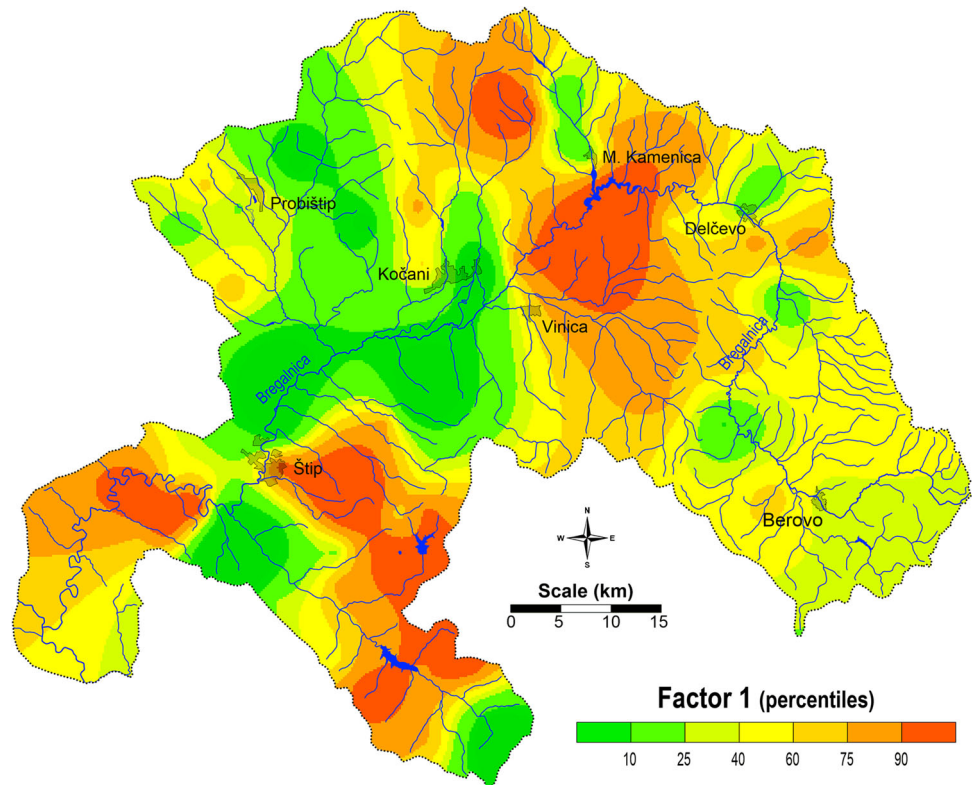
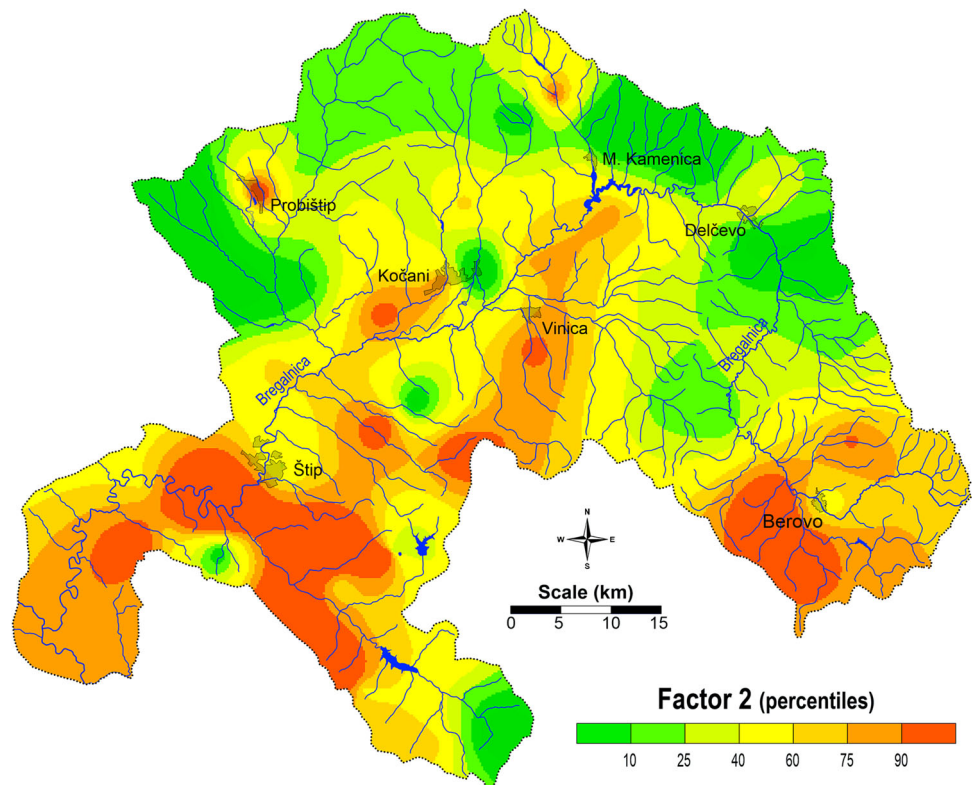


**Fig. 8** Distribution patterns for *Factor 2* Be–Cr–Li–Mg–Ni



As–Co–Ge–V distribution can be used as a proposed mechanism for possible tracking of anthropogenic poly-metallic enrichments (Fig. 12).

Factor 6 includes K–Na–Sc–Ti. Although it is the least distinguished factor; nevertheless this geochemical association is related to the lithogenic dominance of the

**Fig. 9** Distribution patterns for *Factor 3* Ag–Bi–Cd–Cu–In–Mn–Pb–Sb–Te–W–Zn

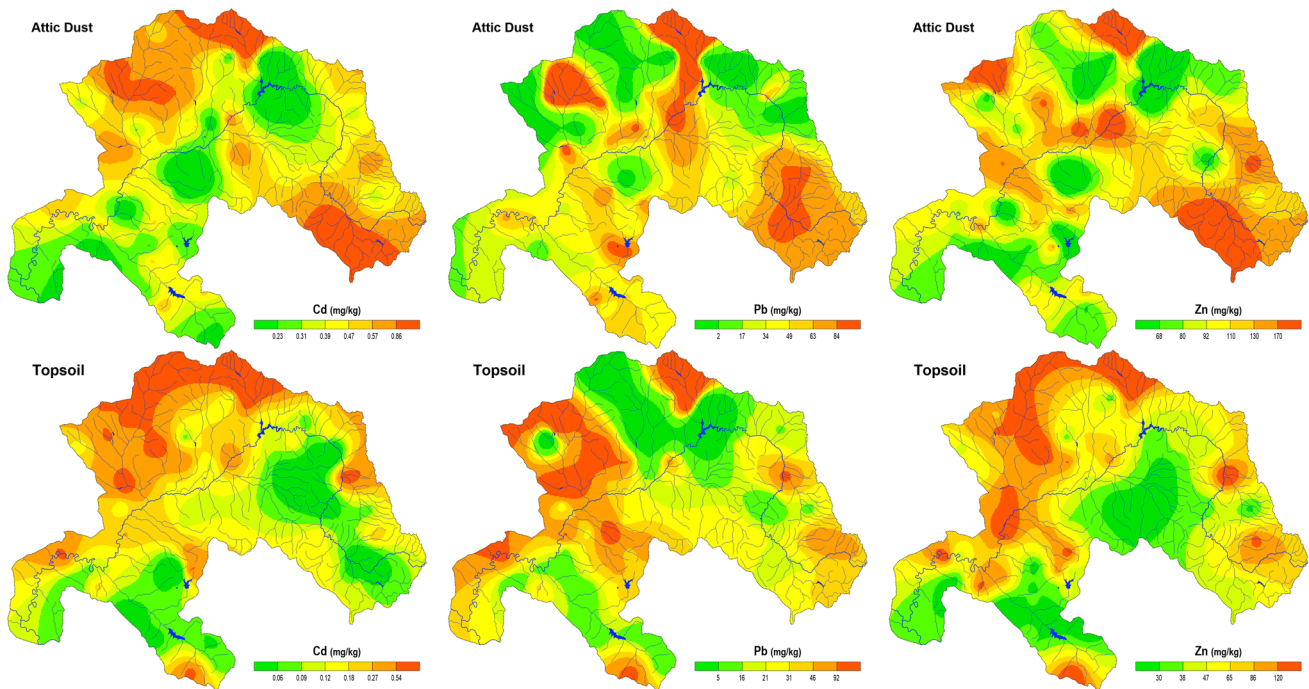
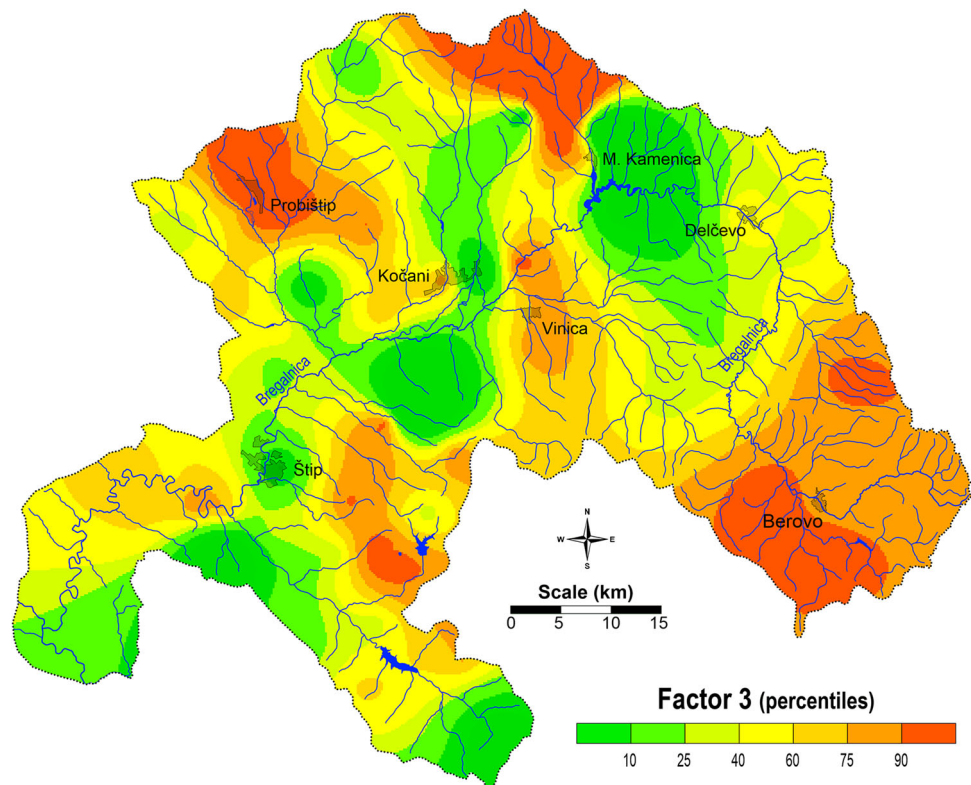


**Fig. 10** Distribution patterns for Cd, Pb and Zn (in attic dust and surface soil)

Neogene sediments and Paleogene flysch, as illustrated in Fig. 6. Their occurrence in the environment is usually correlated to the major minerals in basaltic and

ultramafic rocks that have two kinds of cationic lattice sites: small tetrahedral sites occupied by Si and Al (White 2013). As a result of their solubility they are



**Fig. 11** Distribution patterns for *Factor 4* Ba–Cs–Hf–Pd–Rb–Sr–Tl–Zr

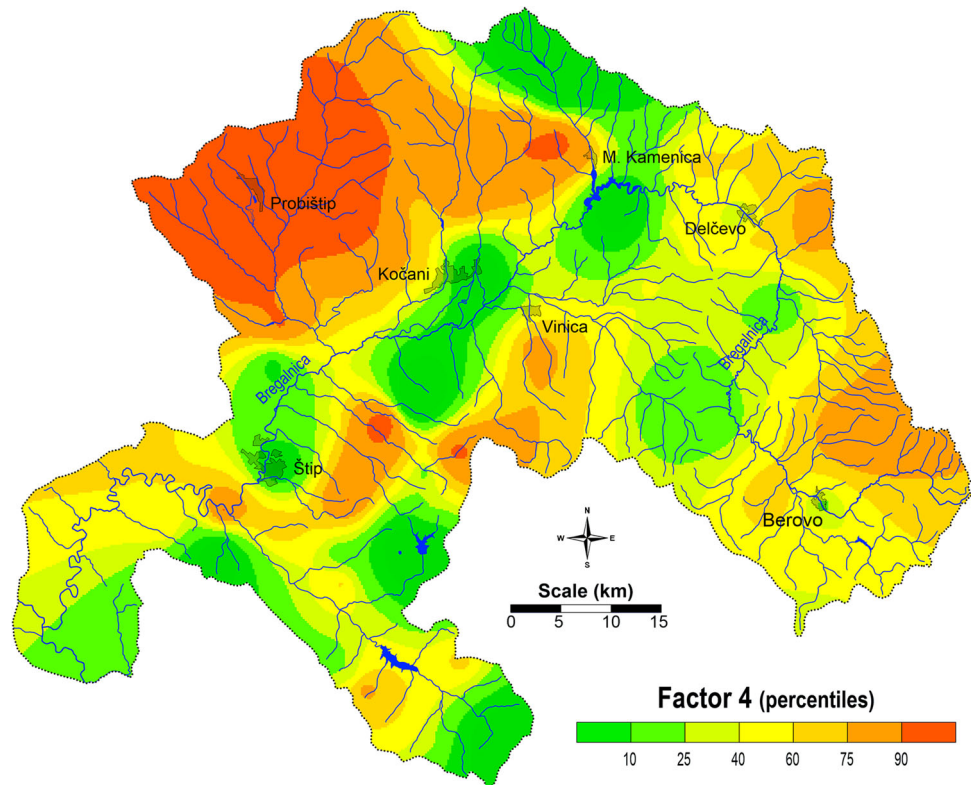
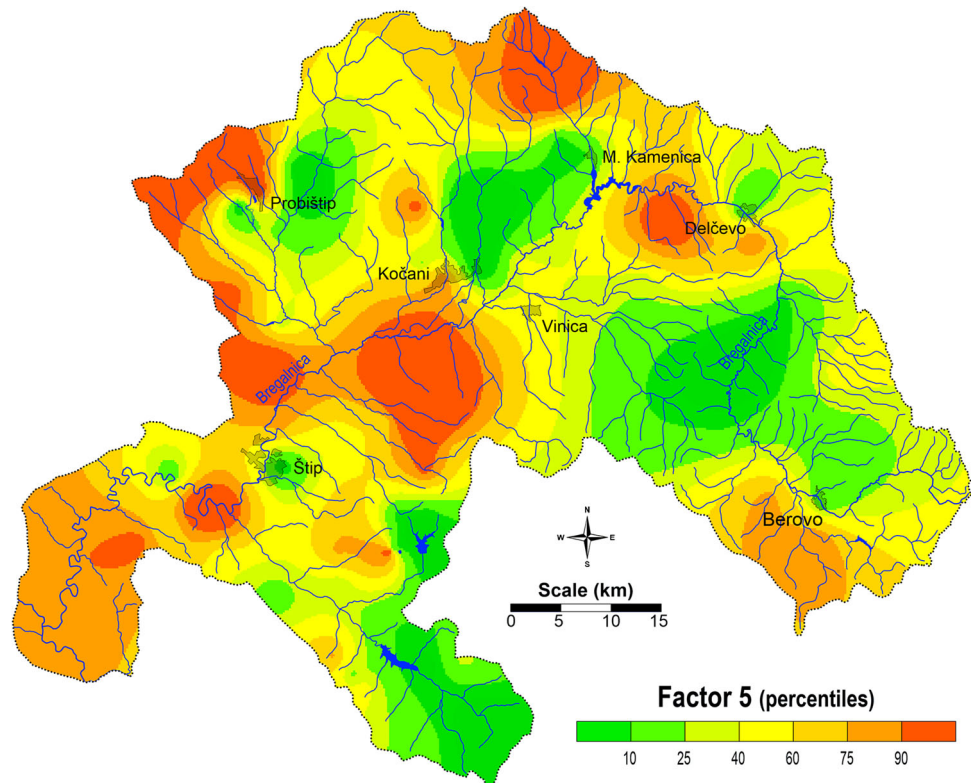


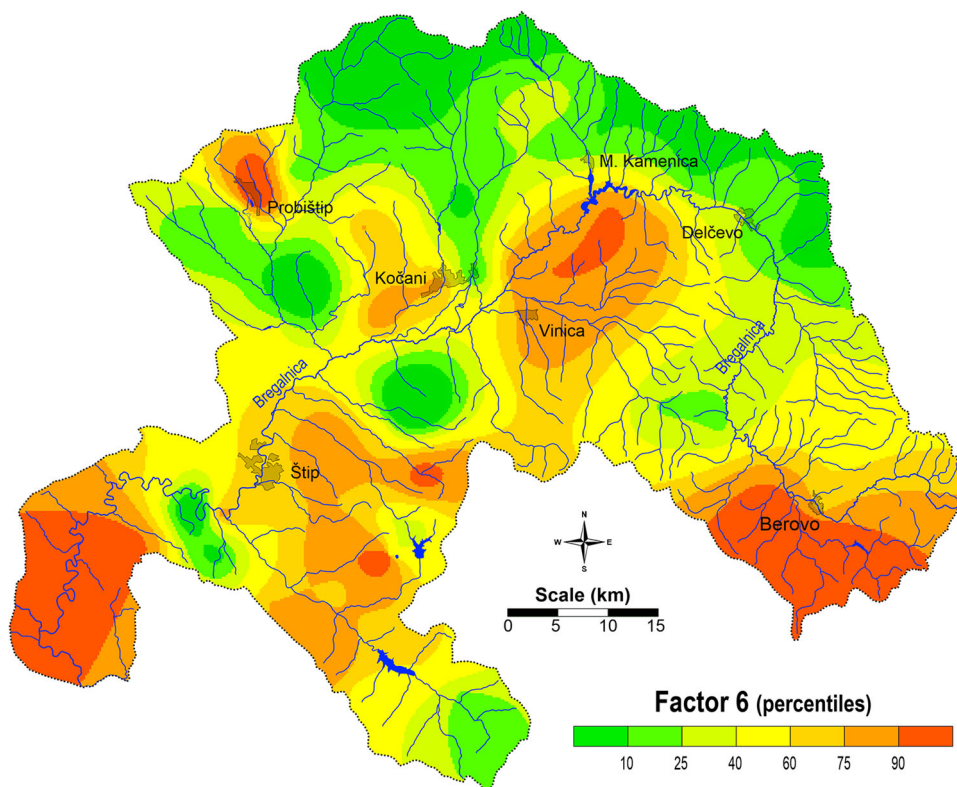
**Fig. 12** Distribution patterns for *Factor 5* As–Co–Ge–V



quite mobile during metamorphism and weathering. Basic hotspots were correlated with the sedimentary mineralisation along the whole course of the Bregalnica

River terraces. Quaternary terraces in Kočani valley are also marked with this lithogenic marker (Fig. 13).

**Fig. 13** Distribution patterns for *Factor 6* K–Na–Sc–Ti



## Conclusions

The present investigation points to a strong correlation between the lithogenic and anthropogenic atmospheric distribution of 69 elements in dust deposited in attics. This environmental media contain a mixture of material derived from in situ weathering of parent material and atmospheric input dominated by continental dust. The anthropogenic activities of poly-metallic hydrothermal exploitation (Sasa, Zletovo, and Bučim mines) performed in certain areas leads to increased content of certain heavy metals in the atmosphere. Statistical factor analysis singled out one dominant anthropogenic group of elements (Ag–Bi–Cd–Cu–In–Mn–Pb–Sb–Te–W–Zn). The significant health risk contents were determined in dust deposits for Cd, Pb and Zn (25, 3900, and 3200 mg/kg, respectively). The geochemistry of the As–Co–Ge–V was assumed as secondary consequence of anthropogenic emissions and correlated with the dominant lithogenic occurrence of Oligocene and Neogene volcanism. The fine particles from the mining operations are spread in the atmosphere by the wind. Excluding the possibility of physical erosion and decrease of dust input, chemical weathering may result in a loss of dust and lead to underestimation of the time-averaged dust deposition rates at the old sites. The dominant lithogenic markers that characterised the investigated area were extracted as follows: Ga–Nb–Ta–Y–(La–Gd)–(Eu–Lu), Ba–Cs–Hf–Pd–Rb–Sr–Tl–Zr, and K–Na–Sc–Ti. The attic

dust/soils analysis implies the significant influence of continental dust.

Future work will allow refinement and more precise fingerprinting of geochemical processes, including the role of dust emissions and trace element-enriched accessory minerals in metasomatic events. Also, experiments are needed to extend the partition coefficient determinations to higher assurance levels in order to resolve controversies over geochemical evolution.

**Acknowledgements** This work was funded by Core Program, under the support of ANCSI, Project No. PN16.40.02.01.

## References

- Ajmone-Marsan F, Biasioli M, Kralj T, Grčman H, Davidson CM, Hursthouse AS et al (2008) Metals in particle-size fractions of the soils of five European cities. *Environ Pollut* 152(1):73–81
- Alijagić J (2008) Distribution of chemical elements in an old metallurgic area, Zenica (Central Bosnia) (MSc thesis) Faculty of Science, Masaryk University, Brno
- Alijagić J, Šajn R (2011) Distribution of chemical elements in an old metallurgical area, Zenica (Bosnia and Herzegovina). *Geoderma* 162(1):71–85
- Angelovska S, Stafilov T, Šajn R, Balabanova B (2016) Geogenic and anthropogenic moss responsiveness to element distribution around a Pb–Zn mine, Toranica, Republic of Macedonia. *Arch Environ Contam Toxicol* 70(3):487–505
- Arsovski M (1997) Tectonics of Macedonia. Faculty of Mining and Geology, Štip, pp 1–306

- Bačeva K, Stafilov T, Šajn R (2012) Monitoring of air pollution with heavy metals in the vicinity of ferronickel smelter plant by deposited dust. *Maced J Ecol Environ* 1(1–2):17–24
- Balabanova B, Stafilov T, Bačeva K, Šajn R (2010) Biomonitoring of atmospheric pollution with heavy metals in the copper mine vicinity located near Radoviš, Republic of Macedonia. *J Environ Sci Health A* 45:1504–1518
- Balabanova B, Stafilov T, Šajn R, Bačeva K (2011) Distribution of chemical elements in attic dust as reflection of their geogenic and anthropogenic sources in the vicinity of the copper mine and flotation plant. *Arch Environ Contam Toxicol* 61(2):173–184
- Balabanova B, Stafilov T, Šajn R, Bačeva K (2012) Characterisation of heavy metals in lichen species *Hypogymnia physodes* and *Evernia prunastri* due to biomonitoring of air pollution in the vicinity of copper mine. *Int J Environ Res* 6(3):779–794
- Balabanova B, Stafilov T, Šajn R, Bačeva K (2014) Comparison of response of moss, lichens and attic dust to geology and atmospheric pollution from copper mine. *Int J Environ Sci Technol* 11:517–528
- Balabanova B, Stafilov T, Šajn R (2015) Lithological distribution of rare earth elements in automorphic and alluvial soils in the Bregalnica river basin. *Maced J Chem Chem Eng* 34(1):201–212
- Balabanova B, Stafilov T, Šajn R, Tănăselia (2016) Geochemical hunting of lithogenic and anthropogenic impacts on polymetallic distribution (Bregalnica river basin, Republic of Macedonia). *J Environ Sci Health A* 51(13):1180–1194
- Barandovski L, Frontasyeva MV, Stafilov T, Šajn R, Ostrovnyaya TM (2015) Multi-element atmospheric deposition in Macedonia studied by the moss biomonitoring technique. *Environ Sci Pollut Res* 22(20):6077–6097
- Beelen R, Hoek G, Pebesma E, Vienneau D, de Hoogh K, Briggs DJ (2009) Mapping of background air pollution at a fine spatial scale across the European Union. *Sci Total Environ* 407(6):1852–1867
- Bourennane H, Douay F, Sterckeman T, Villanneau E, Ciesielski H, King D, Baize D (2010) Mapping of anthropogenic trace elements inputs in agricultural topsoil from Northern France using enrichment factors. *Geoderma* 157(3):165–174
- Box GE, Cox DR (1964) An analysis of transformations. *J R Stat Soc B* 26(2):211–252
- Cizdziel JV, Hodge VF (2000) Attics as archives for house infiltrating pollutants: trace elements and pesticides in attic dust and soil from southern Nevada and Utah. *Microchem J* 64(1):85–92
- Cizdziel JV, Hodge VF, Faller SH (1998) Plutonium anomalies in attic dust and soils at locations surrounding the Nevada test site. *Chemosphere* 37(6):1157–1168
- Coronas MV, Bavaresco J, Rocha JAV, Geller AM, Caramão EB, Rodrigues MLK, Vargas VMF (2013) Attic dust assessment near a wood treatment plant: past air pollution and potential exposure. *Ecotoxicol Environ Saf* 95:153–160
- Davis JJ, Gulson BL (2005) Ceiling (attic) dust: a “museum” of contamination and potential hazard. *Environ Res* 99(2):177–194
- De Miguel E, Llamas JF, Chacon E, Mazadiego LF (1999) Sources and pathways of trace elements in urban environments: a multi-elemental qualitative approach. *Sci Total Environ* 235(1):355–357
- Dumurdzanov N, Serafimovski T, Burchfiel BC (2004) Evolution of the Neogene–Pleistocene basins of Macedonia. *Geol Soc Am Bull* 1:1–20
- Finlayson-Pitts BJ, Pitts JN (1999) Chemistry of the upper and lower atmosphere: theory, experiments, and applications. Academic press, San Diego
- Fordyce FM, Brown SE, Ander EL, Rawlins BG, O’Donnell KE, Lister TR et al (2005) GSUE: urban geochemical mapping in Great Britain. *Geochem Explor Environ A* 5(4):325–336
- Goodarzi F (2006) Assessment of elemental content of feed coal, combustion residues, and stack emitted materials for a Canadian pulverized coal fired power plant, and their possible environmental effect. *Int J Coal Geol* 65:17–25
- Gosar M, Teršič T (2012) Environmental geochemistry studies in the area of Idrija mercury mine, Slovenia. *Environ Geochem Health* 34(1):27–41
- Gosar M, Šajn R, Biester H (2006) Binding of mercury in soils and attic dust in the Idrija mercury mine area (Slovenia). *Sci Total Environ* 369(1):150–162
- Hensley AR, Scott A, Rosenfeld PE, Clark JJJ (2007) Attic dust and human blood samples collected near a former wood treatment facility. *Environ Res* 105(2):194–199
- Ilacqua V, Freeman NC, Fagliano J, Liroy PJ (2003) The historical record of air pollution as defined by attic dust. *Atmos Environ* 37(17):2379–2389
- ISO 14869–1 (2001) Soil quality: Dissolution for the determination of total element content—Part 1: dissolution with hydrofluoric and perchloric acids. International Organization for Standardization, Geneva
- Jemec Aulfič M, Šajn R (2007) Geochemical research of soil and attic dust in Litija area, Slovenia. *Geologija* 50:497–505
- Kabata-Pendias A (2010) Trace elements in soils and plants. CRC Press, Boca Raton
- Keller CB, Schoene B, Barboni M, Samperton KM, Husson JM (2015) Volcanic–plutonic parity and the differentiation of the continental crust. *Nature* 523(7560):301–307
- Lazarevski A (1993) Climate in Macedonia. Kultura, Skopje
- Liroy PJ, Freeman NC, Millette JR (2002) Dust: a metric for use in residential and building exposure assessment and source characterization. *Environ Health Perspect* 110(10):969
- Mulligan CN (2009) Recent advances in the environmental applications of biosurfactants. *Curr Opin Colloid Interface Sci* 14(5):372–378
- Neff JC, Ballantyne AP, Farmer GL, Mahowald NM, Conroy JL, Landry CC et al (2008) Increasing eolian dust deposition in the western United States linked to human activity. *Nat Geosci* 1(3):189–195
- Pavilonis BT, Liroy PJ, Guazzetti S, Bostick BC, Donna F, Peli M et al (2015) Manganese concentrations in soil and settled dust in an area with historic ferroalloy production. *J Expo Sci Environ Epidemiol* 25(4):443–450
- Popov SI, Stafilov T, Šajn R, Tănăselia C, Bačeva K (2014) Applying of factor analyses for determination of trace elements distribution in water from river Vardar and its tributaries, Macedonia/Greece. *Sci World J* 2014:1–11
- Rakičević T, Dumurdzanov N, Petkovski M (1968) Basic geological map of SFRJ, sheet Štip, M 1:100,000 (map & interpreter). Federal Geological Survey, Belgrade
- Rubatto D (2002) Zircon trace element geochemistry: partitioning with garnet and the link between U–Pb ages and metamorphism. *Chem Geol* 184(1):123–138
- Saeedi M, Li LY, Salmanzadeh M (2012) Heavy metals and polycyclic aromatic hydrocarbons: pollution and ecological risk assessment in street dust of Tehran. *J Hazard Mater* 227:9–17
- Šajn R (2000) Influence of lithology and antropogenic activity on distribution of chemical elements in dwelling dust, Slovenia. *Geologija* 43:85–101
- Šajn R (2001) Geochemical research of soil and attic dust in Celje area (Slovenia). *Geologija* 44:351–362
- Šajn R (2002) Influence of mining and metallurgy on chemical composition of soil and attic dust in Meža valley, Slovenia. *Geologija* 45:547–552
- Šajn R (2003) Distribution of chemical elements in attic dust and soil as reflection of lithology and anthropogenic influence in Slovenia. *J de Phys* 107:1173–1176
- Šajn R (2005) Using attic dust and soil for the separation of anthropogenic and geogenic elemental distributions in an old metallurgic area (Celje, Slovenia). *Geochemistry* 5:59–67

- Šajn R (2006) Factor analysis of soil and attic-dust to separatemining and metallurgy influence, Meza valley, Slovenia. *Math Geol* 38:735–746
- Salminen R, Batista MJ, Bidovec M, Demetriades A, De Vivo B, De Vos W et al (2005) FOREGS geochemical atlas of Europe. Part 1: background information, methodology and maps. (<http://weppi.gtk.fi/publ/foregsatlas>)
- Serafimovski T, Tasev G (2003) The Zletovo subvolcanic hydrothermal Pb–Zn mineral deposit in the Republic of Macedonia. In: Geodynamics and ore deposit evolution of the Alpine–Balkan–Carpathian–Dinaride Province. Final GEODE-ABCD Workshop. Programme and Abstracts. Seggau, Austria, pp 22–24
- Stafilov T (2014) Environmental pollution with heavy metals in the Republic of Macedonia. *Contrib Sect Nat Math Biotech Sci MASA* 35(2):81–119
- Stafilov T, Šajn R, Pančevski Z, Boev B, Frontasyeva MV, Strelkova LP (2010) Heavy metal contamination of topsoils around a lead and zinc smelter in the Republic of Macedonia. *J Hazard Mater* 175(1):896–914
- Stafilov T, Šajn R, Balabanova B, Bačeva K (2012) Distribution of heavy metals in attic and deposited dust in the vicinity of copper ore processing and ferronickel smelter plants in the Republic of Macedonia. *Dust Sources, Environmental Concerns and Control*. Nova Science Publishers, Inc., New York, pp 57–98
- State Statistical Office of Republic of Macedonia (2015) Environmental statistics, Skopje
- Tye AM, Hodgkinson ES, Rawlins BG (2006) Microscopic and chemical studies of metal particulates in tree bark and attic dust: evidence for historical atmospheric smelter emissions, Humber-side, UK. *J Environ Monit* 8(9):904–912
- Völgyesi P, Jordan G, Zacháry D, Szabó C, Bartha A, Matschullat J (2014) Attic dust reflects long-term airborne contamination of an industrial area: a case study from Ajka, Hungary. *Appl Geochem* 46:19–29
- Vrhovnik P, Smuc NR, Dolenc T, Serafimovski T, Dolenc M (2013) Impact of Pb–Zn mining activity on surficial sediments of Lake Kalimanci (FYR Macedonia). *Turk J Earth Sci* 22(6): 996–1009
- White WM (2013) *Geochemistry*. Wiley, New York
- Wong CS, Li X, Thornton I (2006) Urban environmental geochemistry of trace metals. *Environ Pollut* 142(1):1–16
- Žibret G (2008) Determination of historical emission of heavy metals into the atmosphere: celje case study. *Environ Geol* 56(1):189–196
- Žibret G, Šajn R (2008) Modelling of atmospheric dispersion of heavy metals in the Celje area, Slovenia. *J Geochem Explor* 97(1):29–41
- Žibret G, Šajn R (2010) Hunting for geochemical associations of elements: factor analysis and self-organising maps. *Math Geosci* 42:681–703